

Modelling compaction variability in out-of-autoclave prepreg laminate

Daria Bontch-Osmolovskaia¹, Xuesen Zeng², Paul Callus³,
Andrew Rider⁴, Paul Chang⁵ and Peter Schubel⁶

¹ University of Southern Queensland, Centre for Future Materials, Toowoomba, Australia,
Daria.Bontch-Osmolovskaia@usq.edu.au , www.usq.edu.au

² University of Southern Queensland, Centre for Future Materials, Toowoomba, Australia,
Xuesen.Zeng@usq.edu.au

³ Aerospace Division, Defence Science & Technology Group, Melbourne, Australia
Paul.Callus@dst.defence.gov.au , www.dst.defence.gov.au

⁴ Aerospace Division, Defence Science & Technology Group, Melbourne, Australia
Paul.Chang@dst.defence.gov.au

⁵ Aerospace Division, Defence Science & Technology Group, Melbourne, Australia
Andrew.Rider@dst.defence.gov.au

⁶ University of Southern Queensland, Centre for Future Materials, Toowoomba, Australia,
Peter.Schubel@usq.edu.au

Keywords: Out-of-autoclave prepreg, porosity / voids, modelling

ABSTRACT

The use of Out-Of-Autoclave (OOA) materials is on the increase in manufacture and repair of aerospace vehicle parts. However, the required aerospace quality standard (sub 1% porosity) is difficult to achieve. This paper proposes a novel experimental method for imaging the flow of trapped air bubbles through the OOA laminate stack. The goal is to quantify the volume of air and volatiles, trapped between the plies during the manufacturing process which will cause the undesirable porosity in the cured part. This paper describes the experimental scanning method for imaging a single ply of OOA material, capable of imaging air bubbles up to 10 microns in size. Then it proposes a future workflow, potentially capable of increasing resolutions of the scans to 3 microns. The air flow is to be modelled numerically, with the goal of constructing an accurate model of a single ply of OOA material – which can be used as a building block in future development of a 3-dimensional model of the laminate stack. This future exploration proposes the use of a novel method, employing a pressure mat during the vacuum consolidation treatment process.

1. INTRODUCTION

Carbon Fibre Reinforced Plastic (CFRP) composite materials are used in manufacture of load-bearing aerospace vehicles. These materials have high specific stiffness and strength; they have low susceptibility to fatigue and corrosion. This directly translates to enhancing the performance of aerospace vehicles and platforms in terms of their speed, payload and range. The aerospace standard for porosity in manufactured parts is < 2% void content [1], which is regularly achieved in the Autoclave manufacturing process. Defects such as porosity and delamination can substantially reduce the mechanical performance. Many processes in aerospace composites manufacturing are directed at keeping these defects within acceptable limits.

Usually, the CFRP parts are manufactured by using Autoclave material systems, cured at 5-7 atm pressure. Another manufacturing option is an Out-Of-Autoclave (OOA) method, which employs a vacuum bag and a relatively low temperature oven cure. However, as the pressure in an OOA process is only 1 atm, this creates a high potential for creation of defects and unacceptable porosity [1, 2].

A common method for repairing composite panels in-situ is to manufacture repair patches in the OOA process, and then use adhesives to make the bond between the repair patch and the underlying structure. Machining techniques such as scarf repairs ensure a better connection between the surfaces [3].

The current study aims to improve the reliability of the OOA composite repair process, by integrating advanced sensing technology and imaging techniques. The approach employs a numerical modelling approach to understand the effect of processing parameters (vacuum, humidity, heating regime etc.) on defect formation.

The fibres in the uncured unidirectional (UD) OOA prepreg materials are not fully impregnated with resin, and the plies are designed with continuous resin-free paths along the fibres. These pathways are denoted as ‘engineered vacuum channels’ (EVaCs); they allow migration of gas towards the boundaries of the sample during vacuum bag treatment of the laminate stack. The consolidation process using vacuum bags relies on this microstructure to enable the evacuation of air, moisture and volatile gasses from the laminate. After the vacuum treatment is completed (or if employing super-ambient hold – during the process), the prepreg is cured at higher temperatures, decreasing the viscosity of resin which gradually fills the EVaCs. The goal of OOA method is to gel the resin immediately after the pores are filled, creating a defect-free, fully dense piece.

A substantial amount of research has been directed at creating computational models of compaction and resin / air flow [4-8], as well as experimental methods which push the manufacturer’s recommended processing window, such as using super-dwell conditions to significantly decrease the required vacuum treatment time [9]. However, there are some limitations evident in the existing literature. One of these is exploration of small samples of the material, with Kim [8] using samples sized 25 mm square, and Hu [10] – 127 mm square. This study is motivated by a need for understanding the behaviour of this prepreg material in application of real-world repair patches, which should about 280-300 mm square. Another limitation is the complexity of existing compaction models, such as Helmus [4, 5, 11] or Matveev [12]. This study is driven by the need for a simplified model that can be used to predict the behaviour of air voids transfer through the EVaCs during vacuum and heat treatment (debulking) out of a laminate stack.

This study is the first step in modelling compaction and air evacuation from the laminate stack, supported by the state-of-the-art sensor and imaging equipment, aimed at explaining experimentally measured variability in a cured aerospace grade out-of-autoclave prepreg laminate stack.

2. EXPERIMENTAL METHOD

2.1. Materials

The study uses an out-of-autoclave prepreg system from Solvay – CYCOM 5320-1/IM7 12K 145gsm 49-inch wide unidirectional fabric, with 33% resin content by weight.

For the feasibility study, 290 mm x 290 mm laminate was hand laid up with a 30-ply stacking sequence of [45 0 0 -45 90]_{3s}. The laminate stack, prior to consolidation, was 5.29 mm thick consisting of 44% volume fraction fibre, 30% volume fraction resin, and 26% volume fraction air. The fully cured laminate had a thickness of 3.9 mm, with 60% volume fraction fibre and 40% volume fraction resin.

2.2. Methodology Workflow

The workflow of methodology is shown graphically on Fig. 1. This stage of the project is aimed at characterising a single ply of the material, including the flow of trapped air voids through the EVaCs, both under vacuum and heat treatment. It is intended to use this single ply model as a building block in the future model of a full laminate stack (20 to 30 plies), to model and characterise the compaction behaviour. The ultimate goal is to simulate and characterise formation (and prevention) of porosity-related defects in the laminate stack.

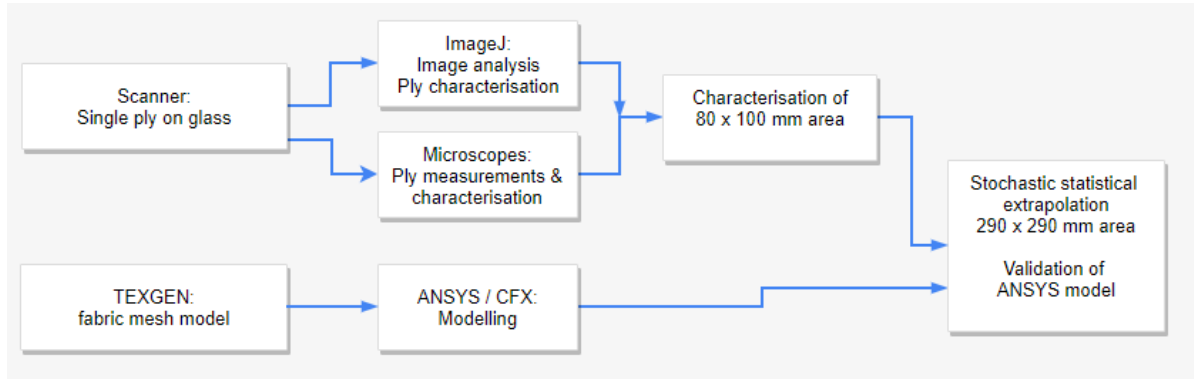


Figure 1 - Methodology workflow diagram

2.3. Imaging of a Single Ply

To understand the compaction behaviour of the material, the first stage of the study is focused on characterising a single ply of the material. The goal is to understand and quantify the average volume and distribution of voids between the plies in a laminate stack, created in the layup process. A single ply of the material was imaged, and the results used to characterise the ply and distribution of voids, and to serve as the foundation for the numerical model.

A single ply of the material was adhered to glass plates of varying thickness (2 – 6 mm, clear tempered glass with and without coating) and explored with various scanning techniques. Glass plates provided a transparent flat stiff surface to which the prepreg could slowly conform, and be scanned for image analysis. As Hu [10] describes, the entrapped air voids are located in the resin-rich zones between the plies, and therefore precise conditions for reproducing gas entrapment and removal require introduction of a resin film in the layup. However, a film of this type would obscure the scanning equipment, and clarity of scans. Therefore, it was decided to simply use cleaned glass plates.

It was established that image resolution of a high-end photograph scanner (9600 dpi resolution), once calibrated, was sufficient to produce good quality scans of samples. The lighting used by this scanner was diffused, resulting in high quality images.

The scanner and a scanning sample on a glass plate are shown on Fig. 1.

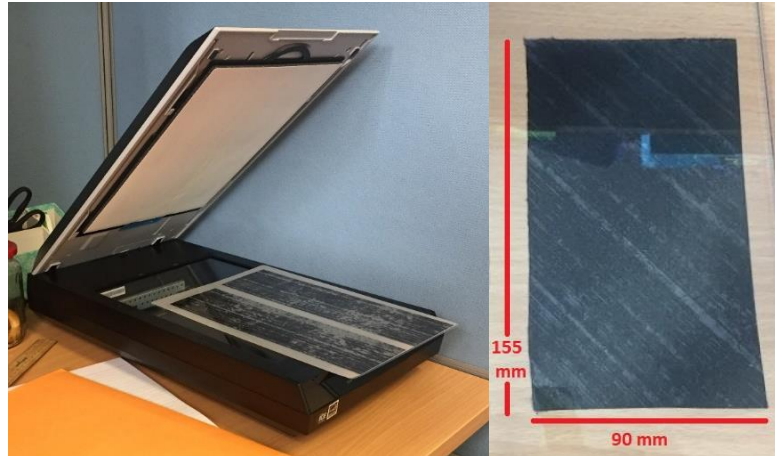


Figure 2 - Scanner (EPSON Perfection V550) and samples on 6 mm glass plate

To establish the reference dimensions for image processing software (ImageJ), a scanning electron microscope (JEOL JCM-6000) and stereo microscope with camera (SMZ-168 with Olympus XC10 camera) were used.

After scanning the samples, the images were imported into ImageJ software for analysis. The goal of this analysis is to develop a method for quantifying the area of air bubbles (which will act as potential voids in the cured prepreg) trapped between the glass plate and the prepreg ply. The full repair patch size is 290x290 mm, however the scanner set on high resolution is limited to 21,000 x 30,000 pixels – approximately 80 x 100mm. Therefore, this experiment requires scanning and analysis of a significant number of samples to provide a reliable population size for further analysis.

The next stage of this analysis requires installation of the scanner under the vacuum bag setup, to enable periodic scanning of the ply as its undergoing vacuum bag treatment. It is envisaged that this will provide valuable data for imaging de-bulking of a single prepreg ply in vacuum. This data could provide information about the real-time flow rate of air through the EVaCs, and the expected residual volumes of voids post-vacuum treatment.

The scanner and vacuum bag set up is shown schematically on Fig. 3.

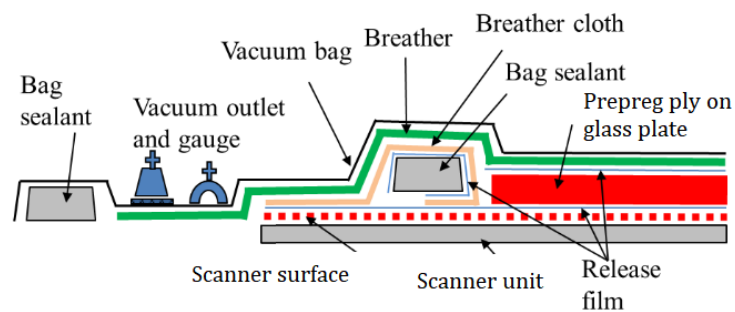


Figure 3 - Scanner setup schematic with vacuum bag

3. NUMERICAL MODELLING

The compaction behaviour of the OOA prepreg is governed by a viscoelastic relationship between resin and fibre, and the compressible behaviour of entrapped air. The proposed modelling method is based on a mesoscale unit cell with stochastic variability of entrapped air pockets. A model of a single layer of OOA prepreg is illustrated on Fig. 4.

3.1. Fundamental Modelling Equations

The permeability of the material ply, parallel to the yarn axes, is depending on the permeability of the axial yarn itself, and the inter-yarn gaps. Endruiweit [13] proposes that it can be approximated by the application of a rule of mixtures, where the fraction of the layer cross-sectional area is occupied by gaps Φ . Then, the axial layer permeability K_l can be approximated as

$$K_l = \Phi K_g + (1 - \Phi) K_y \quad (1)$$

where K_g is the equivalent axial gap permeability and K_y is the axial yarn permeability.

Then, if the cross-sectional area of the yarn is A_y , and the total cross-sectional area is A_{UC} , the fraction of the total cross-sectional layer area, occupied by the gap is

$$\Phi = 1 - \frac{A_y}{A_{UC}} \quad (2)$$

The cross-sectional shape of the yarn is determined by the effects of through-thickness and lateral compression [13], and the cross-section can be approximated by a power ellipsoidal shape, described by points (x, y) , which satisfy the equation

$$\left(\frac{x}{R}\right)^2 + \left(\frac{2y}{h}\right)^{\frac{2}{n}} = 1 \quad (3)$$

where n describes the shape of the power ellipse, $2R$ is the yarn width, and h is the yarn height.

A fully developed laminar flow of an incompressible fluid through a pipe with constant cross-section is described by the Navier-Stokes equations, reduced to the Poisson form:

$$\frac{\partial^2 u}{\partial x^2} + \frac{\partial^2 u}{\partial y^2} = \frac{1}{\eta} \frac{\Delta p}{L} \quad (4)$$

where $u(x,y)$ is the local flow velocity in axial direction, η is the fluid viscosity, L is the length of pipe, and Δp is the gradient pressure drop along length L . Taking $u = 0$ at the pipe boundary and numerically solving this equation gives the average axial velocity $v(x,y)$, and with application of Darcy's law for unidirectional flow in a porous medium, the equivalent axial duct permeability K_g can be calculated as follows.

$$K_g = \frac{v\eta L}{\Delta p} \quad (5)$$

The pressure loss in a viscous flow along a hydraulic pipe can be described by Darcy-Weisbach equation, determining the equivalent permeability as

$$K_g = \frac{2D_h^2}{c} \quad (6)$$

where c is a shape factor, corresponding to four-times the Poiseuille number, and D_h is the hydraulic diameter of the gap, described as:

$$D_h = \frac{4A_g}{P_g} \quad (7)$$

where A_g is the gap cross-sectional area, and P_g is perimeter of the gap cross-section [13].

The shape factor c can also be defined as a product of the Darcy friction factor,

$$f_D = \frac{2D_h \Delta p}{\rho_f v^2 L} \quad (8)$$

where ρ_f is the fluid density. This equation determines the ratio between the local density of kinetic energy, local shear stress and the Reynolds number (the ratio of inertial and viscous forces),

$$Re = \frac{\rho_f v D_h}{\eta} \quad (9)$$

As described by Endruiweit [13], the value of c provides as measure for the effect of viscous friction on flux. The goal of these calculations is to predict the equivalent gap permeability for a power-elliptical cross-sectional shape of a yarn (including UD tape used in this project).

Ultimately, the goal is to model the flow of air as a fluid through the EVaCs, filled with viscous resin, thus describing the flow of trapped voids out of the laminate stack during vacuum treatment. This would allow prediction of the trapped air volume in a laminate part, which could become porous defects in a cured part.

3.2. Modelling method

The goal of the numerical model in this project is to analyze flow behavior of air-filled voids through the resin and out of the laminate stack.

To achieve this goal, a 3D mesh model of the UD tape is created in textile modelling software package (TexGen). For the first iteration of the model, an idealized placement was considered, with two widths equal to 3650 μm and EVaC gaps 250 μm , as determined from measuring the scans (see Results section). The domain, surrounding the tows, was used to represent trapped air around a prepreg ply.

The geometric model is shown on Fig. 4.

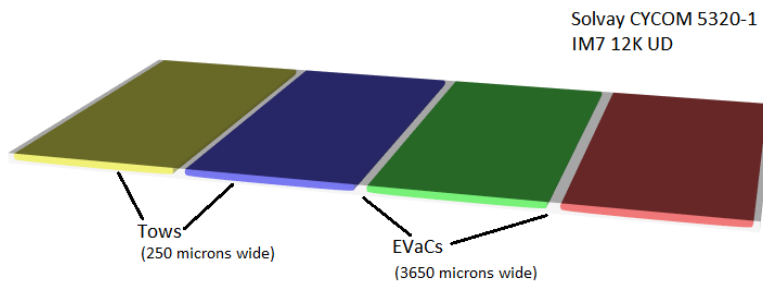


Figure 4 - Single ply mesh model (TexGen)

The mesh model will then imported into ANSYS CFX package for modelling fluid flow of trapped air through the EVaCs and the surface of the tows. The workflow for modelling air flow is shown in Fig. 5.

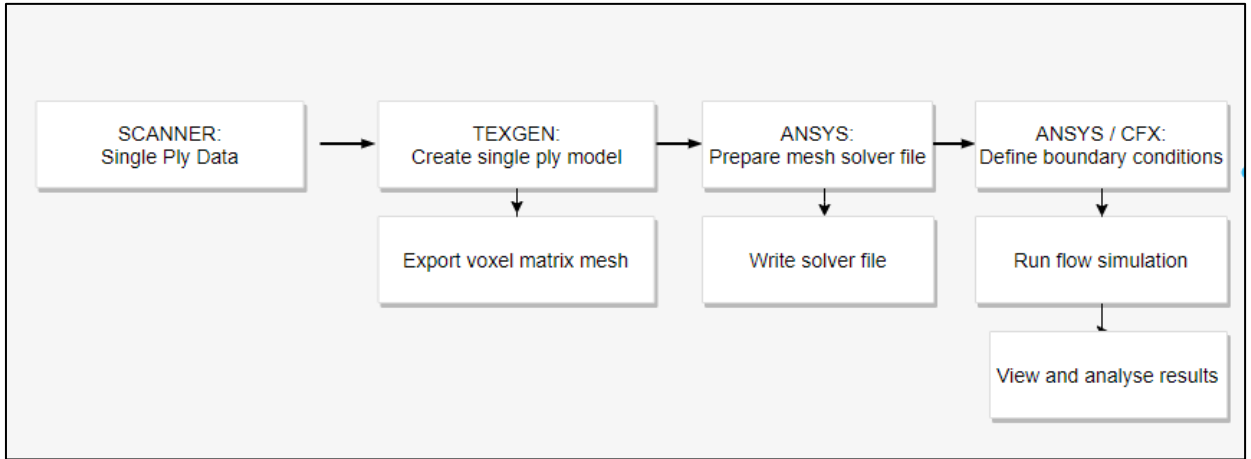


Figure 5 – Flowchart for modelling air flow, based on [14]

In the future, it is planned to extend the model from a single-ply layer to a full laminate stack (20 and 30 layers for thin / thick parts). This will model air flow in-plane through the EVaCs, between the plies and – potentially – with consideration to the out-of-plane air void flow.

4. RESULTS AND DISCUSSION

The results were obtained from scanned images of a single ply, using the desktop scanner and electronic microscopes.

A close up view of a ply, under microscope magnification, is shown on Fig. 6. This image clearly shows EVaCs defined as thick vertical bands. Trapped air voids between the tow and the glass plate are also clearly visible, as small bubbles. The EVaC channels are clearly not continuous. This is particularly clear on the right-hand-side EVaC, where the air bubble is not a continuous ‘column’, as was expected. This could indicate that, during vacuum treatment, some air might not be able to escape through this particular channel – it would be trapped inside the stack, causing porosity in the finished part. This indicates a need for exploration of the relationship between the discontinuous nature of the EVaCs, required vacuum bag pressure and the porosity defects in a finished laminate part.

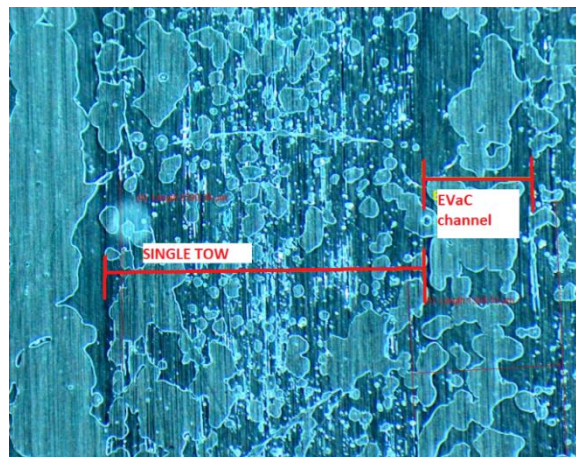


Figure 6 – A single ply under microscope magnification.

It was established that the average width of the tows in the uncompressed UD tape was 3650 ± 25 μm , and the width of EVaCs was 250 ± 25 μm . These measurements were used for preliminary analysis and developing the modelling process flow, until the time when more precise measurements can be obtained.

The depth of the EVaCs cannot be measured with 2D scanning. Further, the profile of the EVaCs presents as slightly rounded, with edges of the tows compacted and no clear depth visible (Fig. 6).

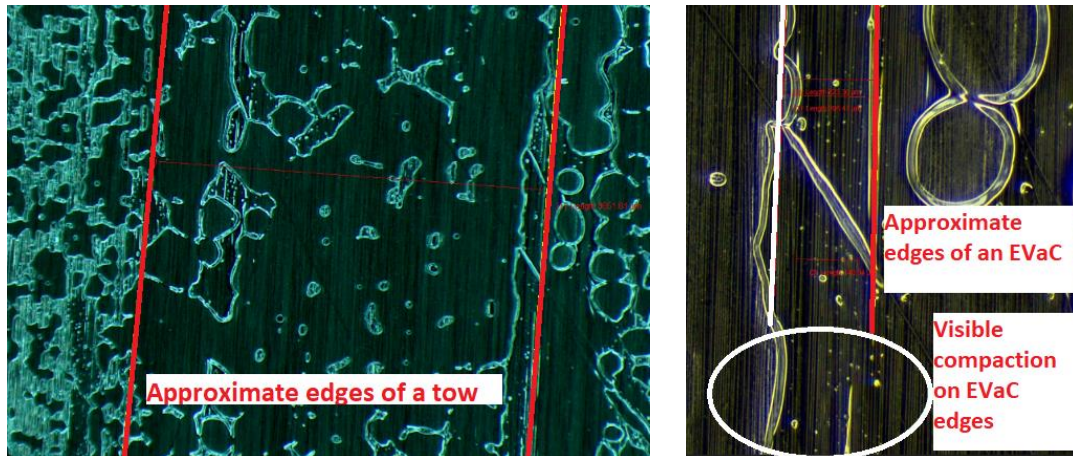


Figure 7 - A single tow under high magnification (microscope). Edges of the tow are shown. Trapped air bubbles are clearly visible.

Using the current scanner setup has imaged the ply reasonably well. The scans are clear, and show a wide range of trapped air bubbles, both inter- and intra-ply. The quality of the images will be improved with further calibration of the scanner focal depth.

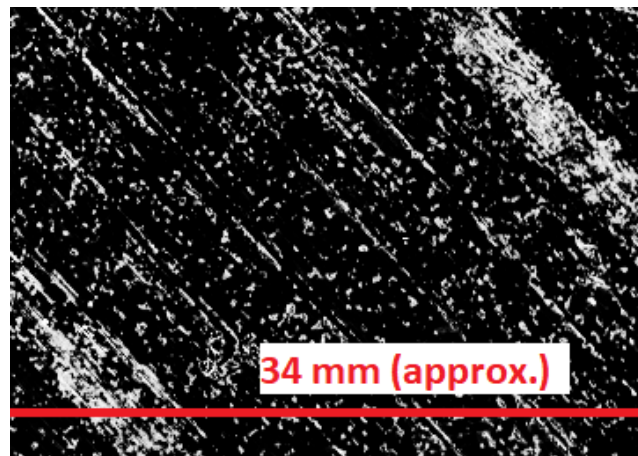


Figure 8- Scan of a ply, showing trapped inter- and intra-ply voids

Currently, the smallest visible trapped air bubble is about 10 μm across. However, the best resolution for 3D samples available with X-ray computed microtomography (or micro-CT) in Australian facilities is about 3 μm . The scanner calibrated to scan at 9600 dpi resolution is potentially capable of obtaining this level of detail, with further calibration. Scans, treated for analysis in ImageJ, are shown on Fig. 9.

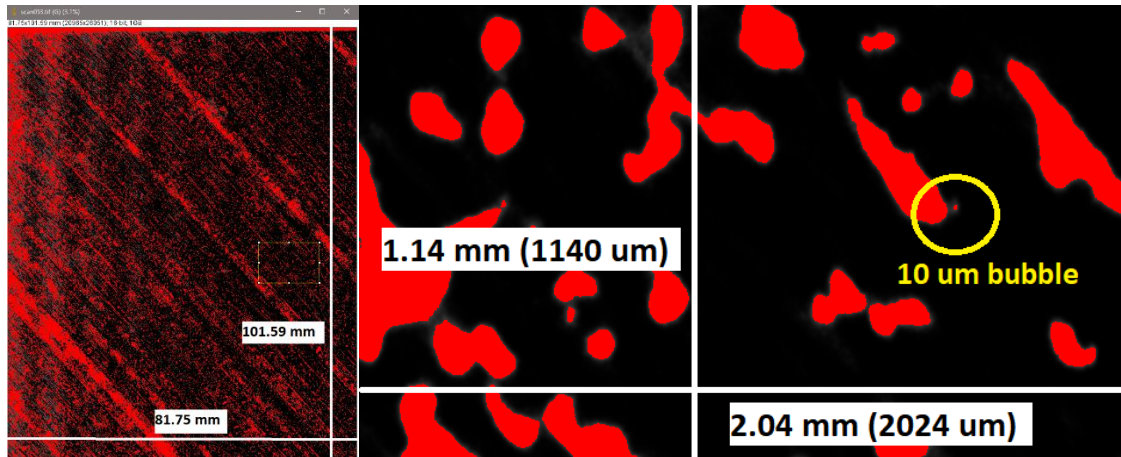


Figure 9 - High resolution scan (81.75 x 101.59 mm real size, 3% zoom) in ImageJ, ready for processing, and 100% zoom of the same.

The project feasibility study [15] employed a high resolution and high accuracy grid of elastomer capacitive tactels for real-time pressure imaging of OOA processes. The pressure mat has a spatial resolution of 2.54 mm, with 16,384 sensors over an area of 32.5 x 32.5 cm. The calibration accuracy of pressure measurement is 0.5%.

The real-time pressure monitoring for the out-of-autoclave prepreg laminate during feasibility study is shown on Fig. 3.

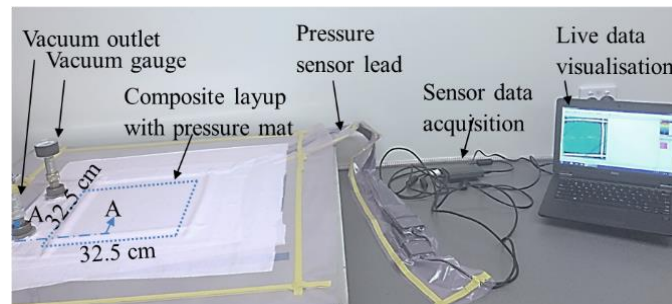


Figure 10 - Process pressure mapping setup for prepreg VBO processing (courtesy of Dr. Zeng)

The data from this process will be used as a foundation for modelling, used to explain the measured compaction variability shown in Fig 11.

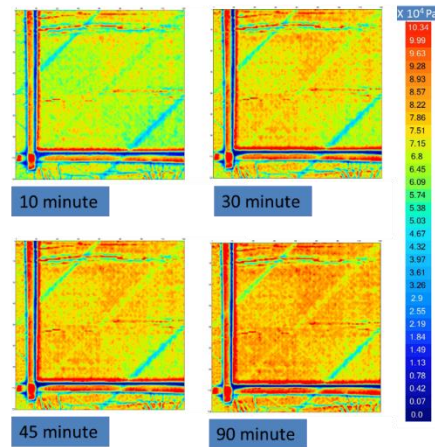


Figure 11 - Time and space dependent pressure distribution in an OOA prepreg laminate consolidated in accordance with manufacturers specifications (courtesy of Dr. Zeng)

5. CONCLUSIONS AND FURTHER WORK

For the final stages of the single-ply characterisation part of the project, the scanner will be recalibrated to obtain 3 micron resolution (if possible), and the glass plates with adhered material ply will be scanned while subjected to vacuum treatment. It is expected that the same plates will be subjected to subsequent heat treatment (super-ambient dwell conditions, based on [9]), to characterise the changes in resin viscosity and its effect on debulking and final porosity of the cured part.

If successful, the next stage of the exploration will be employing micro-CT scanning techniques to image the distribution of air voids inside a 3-dimensional laminate stack. The relationship between the compaction of the full stack and pressure distribution during vacuum treatment will be explored with the help of pressure sensor mat, used during the feasibility study.

6. REFERENCES

- [1] Centea T, Grunefelder LK, Nutt SR. A review of out-of-autoclave prepreps – Material properties, process phenomena, and manufacturing considerations. *Composites Part A: Applied Science and Manufacturing*. 2015;70:132-54.
- [2] Hubert P, Centea T, Grunefelder L, Nutt S, Kratz J, Levy A. 2.4 Out-of-Autoclave Prepreg Processing. In: Beaumont PWR, Zweben CH, editors. *Comprehensive Composite Materials II*. Oxford: Elsevier; 2018. p. 63-94.
- [3] Breitzman TD, Iarve EV, Cook BM, Schoepner GA, Lipton RP. Optimization of a composite scarf repair patch under tensile loading. 2009;40(12):1921-30.
- [4] Helmus R, Kratz J, Potter K, Hubert P, Hinterhölzl R. An experimental technique to characterize interply void formation in unidirectional prepreps. *Journal of Composite Materials*. 2017;51(5):579-91.
- [5] Helmus R, Centea T, Hubert P, Hinterhölzl R. Out-of-autoclave prepreg consolidation: Coupled air evacuation and prepreg impregnation modeling. *Journal of Composite Materials*. 2016;50(10):1403-13.
- [6] Kim D, Centea T, Nutt SR. Modelling and monitoring of out-time and moisture absorption effects on cure kinetics and viscosity for an out-of-autoclave (OoA) prepreg. *Composites Science and Technology*. 2017;138:201-8.
- [7] Kim D, Centea T, Nutt S. In-situ measurement of resin state and cure for efficient non-autoclave manufacturing2015.
- [8] Kim D, Centea T, Nutt SR. Out-time effects on cure kinetics and viscosity for an out-of-autoclave (OOA) prepreg: Modelling and monitoring. *Composites Science and Technology*. 2014;100:63-9.
- [9] Ridgard C. Process selection and optimization for out-of-autoclave prepreg structures2016.

- [10] Hu W, Grunenfelder LK, Centea T, Nutt S. In situ monitoring and analysis of void evolution in unidirectional prepreg. *Journal of Composite Materials*. 2018;52(21):2847-58.
- [11] Helmus R, Hinterhölzl R, Hubert P. A stochastic approach to model material variation determining tow impregnation in out-of-autoclave prepreg consolidation. *Composites Part A: Applied Science and Manufacturing*. 2015;77:293-300.
- [12] Matveev MY, Belnoue JPH, Nixon-Pearson OJ, Ivanov DS, Long AC, Hallett SR, et al. A numerical study of variability in the manufacturing process of thick composite parts. *Composite Structures*. 2019;208:23-32.
- [13] Endruweit A, Zeng X, Matveev M, Long AC. Effect of yarn cross-sectional shape on resin flow through inter-yarn gaps in textile reinforcements. *Composites Part A: Applied Science and Manufacturing*. 2018;104:139-50.
- [14] R Aziz A, Ali M, Zeng X, Umer R, Schubel P, J Cantwell W. Transverse permeability of dry fiber preforms manufactured by automated fiber placement 2017.
- [15] Zeng X, Schubel P. Feasibility Study – Next Generation OOA Composite Repair. Toowoomba: USQ; 2018.